

The physical basis of mollusk shell chiral coiling

Régis Chirat^{a,2}, Alain Goriely^b, and Derek E. Moulton^b

^aCNRS 5276, LGL-TPE, Université Lyon 1, 69622 Villeurbanne Cedex, France; ^bMathematical Institute, University of Oxford, Oxford, UK

This manuscript was compiled on December 4, 2021

1 **Snails are model organisms for studying the genetic, molecular and**
2 **developmental bases of left-right asymmetry in Bilateria. However,**
3 **the development of their typical helicospiral shell, present for the**
4 **last 540 million years in environments as different as the abyss or**
5 **our gardens, remains poorly understood. Conversely, ammonites**
6 **typically have a bilaterally symmetric, planispirally coiled shell, with**
7 **only 1% of 3000 genera displaying either a helicospiral or a mean-**
8 **dering asymmetric shell. A comparative analysis suggests that the**
9 **development of chiral shells in these mollusks is different, and that**
10 **unlike snails, ammonites with asymmetric shells probably had a bi-**
11 **laterally symmetric body diagnostic of cephalopods. We propose a**
12 **mathematical model for the growth of shells, taking into account the**
13 **physical interaction during development between the soft mollusk**
14 **body and its hard shell. Our model shows that a growth mismatch**
15 **between the secreted shell tube and a bilaterally symmetric body in**
16 **ammonites can generate mechanical forces that are balanced by a**
17 **twist of the body, breaking shell symmetry. In gastropods, where a**
18 **twist is intrinsic to the body, the same model predicts that helicospiral**
19 **shells are the most likely shell forms. Our model explains a large**
20 **diversity of forms and shows that although molluscan shells are in-**
21 **crementally secreted at their opening, the path followed by the shell**
22 **edge and the resulting form are partly governed by the mechanics**
23 **of the body inside the shell, a new perspective that explains many**
24 **aspects of their development and evolution.**

coiling | symmetry breaking | chirality | mathematical model | mollusk

1 **A**mong metazoans, Bilateria are organized along an antero-
2 posterior and a dorso-ventral axis that both define the
3 plane of bilateral symmetry, and the left and right sides of the
4 animal. Although bilaterian animals are externally mostly sym-
5 metric, they usually show a consistent left-right asymmetry in
6 internal organs. How left-right symmetry is broken during de-
7 velopment raises fundamental questions, such as the functional
8 implications of asymmetry, defective left-right asymmetry lead-
9 ing to severe pathologies in humans; the developmental stage
10 at which asymmetry is initiated; the dominance in most cases
11 of a given direction (e.g. our heart most often to the left
12 side, liver to the right) rather than a random 50/50 ratio; the
13 extent to which left-right symmetry breaking processes have
14 been evolutionarily conserved among Bilateria; how multilevel
15 asymmetries, from molecular, cellular to organismal level, are
16 related to each other; and how consistent asymmetry is gen-
17 erated in a world where no macroscopic process of chemistry
18 or physics can be used to define unequivocally left from right
19 (1–4).

20 In contrast to most Bilateria, snails display a conspicuous
21 outward asymmetry manifested by a typically dextral (with an
22 opening on the right side when the tip is up) or rarely sinistral
23 helicospiral shell together with marked left-right anatomical
24 asymmetries. The characteristic helicospiral shape of snail
25 shells is a particular kind of chirality, a form being *chiral*
26 if it cannot be superimposed on its mirror image, like our

left and right hands. Shell chirality has intrigued biologists
for centuries, and snails have emerged as model organisms
to address the genetic and developmental bases of left-right
symmetry breaking in Bilateria (5). Chirality in snails is in
direct contrast with the shape of most ammonites*, a group
of extinct mollusk cephalopods with an external chambered
shell that populated the seas for 340 million years and became
extinct 66 million years ago. Like the extant chambered *Nautilus*,
about 99% of 3000 ammonite genera have *non-chiral*,
bilaterally symmetric shells, most often a planispiral or more
rarely a straight shell, or a combination of both forms, despite
the fact that *Nautilus* and gastropods share the same basic
structure of the shell-secreting system (6, 7), and that both
empirical and theoretical evidences suggest it was shared by
ammonites as well (8, 9). That is, ammonites were likely
secreting their shells in the same way as gastropods, and yet
producing in the vast majority of cases symmetric shells. The
remaining 1% of ammonites are represented by some 40 genera
mostly belonging to seven Cretaceous families displaying, at
least during a part of their development, an asymmetric, often
helicospiral shell (10). Two asymmetric genera are also known
in the upper Triassic (11). These rare heteromorph ammonites
display the most stunning shell shapes (Fig. 1), generated
by a combination of different modes of shell coiling during
development. For a long time considered as "aberrant", these
forms have marveled and puzzled paleontologists for years.
In addition to numerous taxonomic studies, special attention
has been paid to the inference of their hydrostratic properties,
lifestyle and paleocology (12–14). However a key question
of developmental biology remains: what are the symmetry-

Significance Statement

A theoretical model suggests that a mechanically induced twist of the soft body underlies the formation of helicospiral shells in snails and ammonites, and also accounts for the startling and unique meandering shells observed in certain species. This theory addresses fundamental developmental issues of chirality and symmetry breaking: in the case of ammonites, how a bilaterally symmetric body can sometimes secrete a non-symmetric shell; for gastropods, how an intrinsic twist possibly due to the asymmetric development of musculature can provide a mechanical motor for generating a chiral shell. Our model highlights the importance of physical forces in biological development, and sheds light on shell coiling in snails, which have been used for a century as model organisms in genetic research.

DEM and RC conceived the study. DEM and AG devised the mathematical model. Computations were performed by DEM. Comparative approach was performed by RC. DEM collected data on shell coiling. All authors contributed to the writing of the paper.

We have no conflict of interest.

²To whom correspondence should be addressed. E-mail: regis.chirat@univ-lyon1.fr

57 breaking processes involved in the development of asymmetric
 58 shells among representatives of a group overwhelmingly char-
 59 acterized by a well-marked bilateral symmetry diagnostic of
 60 the cephalopod body plan?

61 The relative simplicity of the shell growth process in mol-
 62 lusc – an accretionary process occurring at the current shell
 63 opening by the secreting mantle edge – and the diverse and dis-
 64 tinct forms that are generated, as described above, make mol-
 65 lusc an excellent case study for investigating symmetry break-
 66 ing during development, notably in light of recent progress
 67 made in developmental biology on this question in the model
 68 organism, the pond snail *Lymnaea*. Here we present a compar-
 69 ative analysis between gastropods and ammonites and propose
 70 a new unifying model of shell coiling based on the interaction
 71 of the animal’s soft body with its secreted hard shell. Our
 72 model provides a physical explanation for how a bilaterally
 73 symmetric ammonite body may secrete on occasion an asym-
 74 metric shell, and also addresses within the same framework the
 75 ubiquitous formation of helicospiral shells in gastropods, in
 76 light of the exception of bilaterally symmetric shells of limpets.

77 1. Background

78 **A. How snails got their handedness.** A direction of shell coil-
 79 ing in snails is overwhelmingly predominant in a given species
 80 with more than 90% of snails exhibiting dextral shells (15).
 81 For example, only six specimens of sinistral *Cerion* have ever
 82 been found among probably millions of specimens examined
 83 (16). Pond snails of the genus *Lymnaea* have become model
 84 organisms to study the genetic and developmental basis of left-
 85 right asymmetry, leading to a model of maternal inheritance
 86 in which offspring’s handedness is dictated by the mother’s
 87 genotype (17, 18) by a single maternal locus (19). Gastropods
 88 display a spiral cleavage mode of early cell divisions, as do
 89 most representatives of the Lophotrochozoa (one of the three
 90 super-phyyla of Bilateria). The first sign of chirality in snails is
 91 distinguishable in the orientation of the cleavage planes, and
 92 handedness may be defined as early as in the first or second
 93 blastomere divisions. But temporal and spatial cytoskeletal
 94 dynamics for dextral and sinistral embryos are not mirror
 95 images of each other, and show a bias towards dextral forms
 96 from the early stages of spiral cell division (20). Strikingly,
 97 inverting genetically specified third-cleavage directions by me-
 98 chanically altering the relative orientation of cells leads to
 99 snails with inverted handedness, manipulated embryos grow-
 100 ing to ‘dextralized’ sinistral or ‘sinistralized’ dextral snails
 101 (21). This handedness in cleavage acts upstream of the Nodal
 102 signalling pathway long known to be involved in left–right
 103 asymmetry in vertebrates, and involved in snails too (22). In
 104 the quest to discover the long-sought maternally expressed
 105 gene determining handedness, a diaphanous-related formin
 106 gene has been identified (23, 24), providing a proof for the role
 107 of an actin cytoskeleton-regulating protein in determining the
 108 arrangement of blastomeres. In summary, left–right asymme-
 109 try in snails anatomy originates in cellular architecture. The
 110 dynamics of the inherently chiral cytoskeleton governs mechani-
 111 cally the asymmetric behavior of dividing cells at the earliest
 112 stage of development and, ultimately, the body and shell hand-
 113 edness. We will show however that if the link between spiral
 114 cleavage, body and shell handedness is obvious in the model

organism *Lymnaea* (and probably many other gastropods),
 the link between cleavage pattern and helicospiral coiling itself
 is not straightforward and with a single explanation.

B. Ammonites took a weird turn. In contrast to gastropods
 that display a spiral cleavage typical and ancestral of the
 molluscan phylum, cephalopods show a bilateral cleavage. In
 this case, the first cleavage furrow fixates the plane of bilateral
 symmetry of the animal while the second furrow separates
 the future anterior and posterior areas (25). Moreover, unlike
 gastropods, a well-marked bilateral symmetry of the body
 organization both external and internal (e.g. symmetry and
 position of paired organs, such as gills, retractor muscles) is
 a diagnostic feature of the cephalopod body plan (26, 27). A
 bilateral symmetry characterizes also the shell of about 99%
 of ammonite genera, and though their soft body organization
 remains poorly known, muscle attachment marks are also
 bilaterally symmetric (28), unlike those of snails. We also
 know that the embryonic shell (ammonitella) is bilaterally
 symmetric (29), even in heteromorph ammonites with a post-
 embryonic helicospiral shell (30, 31). Moreover, while chirality
 in snails is visible at the earliest embryonic stages, the shell
 of heteromorph ammonites only becomes chiral at a much
 later stage of development, sometimes well after hatching and
 organogenesis, i.e. well after the stage at which the anatomical
 symmetries are established. Note that we reserve the term
 “heteromorph” for species displaying a non-planar shell despite
 the fact that a number of bilaterally symmetric species (but
 with non-overlapping whorls) have been called heteromorphs.

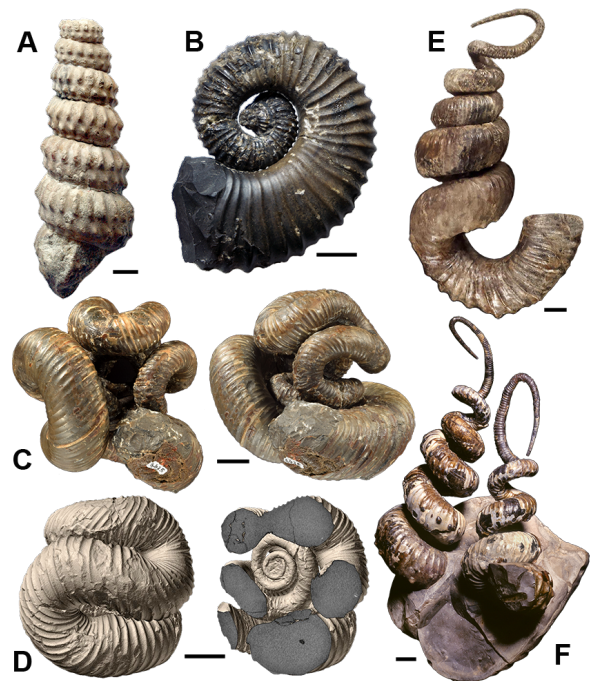


Fig. 1. Heteromorph ammonites with chiral shells. (A) *Turillites costatus* (Cenomanian, France). (B) *Colchidites breistrofferi* (Barremian, Columbia); note the inner helicospiral shell followed by a planispiral stage. (C) *Nipponites mirabilis* (Turonian, Japan). (D) CT scan of a *N. mirabilis* (Upper Cretaceous, Japan) showing the inner planispiral whorls. (E) *Didymoceras stevensoni* (Upper Cretaceous, USA). (F) Two enantiomorphs, sinistral and dextral, of *D. stevensoni* (Upper Cretaceous, USA). (Scale bars, 10 mm. Specimens numbers are given in SI Appendix B).

*When we use the vernacular term “ammonites” we refer to representatives of the cephalopod subclass Ammonoidea.

Heteromorph ammonites with helicospiral shells have

144 evolved repeatedly from ancestors with bilaterally symmet- 205
145 ric, planispiral shells (11, 32, 33). One particularly intriguing 206
146 feature is the modifications of their shell symmetry during 207
147 development (Fig. 1B-F). For example, *Didymoceras*, shown in 208
148 Fig. 1E, displays a bilaterally symmetric shell at the juvenile 209
149 stage (straight or planispiral), a middle growth stage of asym- 210
150 metric, helicospiral shell, and a bilaterally symmetric shell 211
151 portion at maturity. Therefore, the shell shifts from bilaterally 212
152 symmetric to asymmetric and then back to symmetric. It is 213
153 difficult to conceive how the anatomical symmetry of the body 214
154 itself could have shifted in the same way during development. 215
155 In fact, the morphology of the shell in *Didymoceras* (and gen- 216
156 era of other families) shows that during the asymmetric part, 217
157 the ventral side of the shell runs along the longer helicospiral 218
158 and the dorsal side on the shorter one (which results in shell 219
159 edge and ribs oblique to the growth direction), while the left 220
160 and the right sides run along helicospirals of the same length, 221
161 i.e., grow at the same rate as in planispiral shells, contrarily to 222
162 gastropods in which helicospiral shells display a clear left-right 223
163 asymmetry in growth rate. 224

164 In contrast to snails, in which the direction of shell coiling 218
165 is overwhelmingly predominant in a species, a study of about 219
166 1500 specimens of *Didymoceras* shows roughly an equal per- 220
167 centage of dextral and sinistral shells (*D. stevensoni*, n=264, 221
168 d/s ratio: 47/53; *D. nebrascense*, n=882, d/s ratio: 49/51; 222
169 *D. cheyennense*, n=338, d/s ratio: 52/48) (34). This roughly 223
170 50/50 ratio in handedness has also been reported in other 224
171 genera of Nostoceratidae (35, 36), Heteroceratidae (37) or 225
172 Turritidae (38), which suggests that the direction of asym- 226
173 metry was randomly determined and non-heritable. Indeed, 227
174 in the case of asymmetry induced by mechanical twisting, as 228
175 will form the premise of our model, the twisting is equally 229
176 likely to occur in either direction, and the actual observed 230
177 directionality would be determined by ‘noise’ in the system 231
178 and thus unpredictable and non-heritable. Likewise, in the 232
179 known cases of existing Bilateria displaying a random direc- 233
180 tion of asymmetry in some anatomical traits, the direction of 234
181 asymmetry is non-heritable (39). 235

182 The genus *Nipponites* displays some of the most startling 218
183 shapes observed in Nature (Fig. 1C-D). While it seems to 219
184 be irregularly convoluted at first sight, it is not (40) and the 220
185 shell actually follows a precise and reproducible developmental 221
186 sequence. At juvenile stages, *Nipponites* has a planispiral, log- 222
187 arithmically coiled shell with non-overlapping whorls. Then 223
188 the shell unfolds in a succession of meandering oscillations 224
189 on each side of the plane of bilateral symmetry of the first 225
190 planispiral stage, forming alternating dextral and sinistral heli- 226
191 cal sections of increasing wavelength and amplitude. We refer 227
192 to this inversion of handedness as a *perversion* following the 228
193 nomenclature introduced by the mathematician Listing, and 229
194 used by Maxwell and d’Arcy Thompson (41–44). *Nipponites* 230
195 is thought to derive from *Eubostrychoceras* (35), a genus that 231
196 displays bilaterally symmetric planispiral whorls in the early 232
197 stages, a middle growth stage with a helicospiral shell (dextral 233
198 or sinistral in a 50/50 ratio) and a bilaterally symmetric shell 234
199 segment at maturity. An important contribution in the geo- 235
200 metric description of these heteromorph ammonites was made 236
201 by Okamoto (45–47) who showed that these shapes could be 237
202 modeled by varying the curvature and torsion of a centerline 238
203 curve. However, this author assumed that shell coiling was 239
204 controlled by the orientation of these ammonites in the water 240

column through an unknown regulatory mechanism. 205

206 In summary, comparative data present us with a conun- 207
208 drum: unlike snails, evidence suggests that ammonites had a 209
210 bilaterally symmetric body diagnostic of the cephalopod body 211
212 plan but nevertheless sometimes secreted an asymmetric shell. 213
214 Our goal here is to devise a mathematical model that can 215
216 elucidate the developmental mechanism of shell coiling and 217
218 symmetry breaking, and show under what circumstances the 219
220 different shell forms observed in ammonites and gastropods 221
222 can be expected, under what conditions a symmetric body can 223
224 give rise to an asymmetric shell, and how these asymmetric 225
226 shells can change during development. 227

2. Model 217

218 Shell-building mollusks face strong geometric constraints as- 219
220 sociated with accretionary growth of their shell: they secrete 220
221 during their development a shell to which the growing body 221
222 will have to fit in subsequent stages sometimes several months 222
223 or years later. For instance, a mean shell growth rate of 223
224 0.061mm/day in an immature *Nautilus* (48) implies that the 224
225 rear of the growing body may be enclosed in a part of the 225
226 shell tube secreted about 5 years earlier. Our main hypothesis 226
227 is that any growth mismatch between the soft body and the 227
228 secreted shell tube in which it resides can generate mechanical 228
229 stresses balanced by an overall deformation of the body, im- 229
230 pacting the geometry of future secretion. A mismatch between 230
231 different growing parts of an organism plays a fundamental role 231
232 in the genesis of mechanical forces underlying development and 232
233 morphogenesis of plants and animals (49, 50), a mechanism 233
234 involved in molluscan shell morphogenesis as well (8, 9, 51–54). 234
235 That tissue growth and shell growth may be decoupled from 235
236 each other is well known in bivalves and gastropods (55, 56). 236
237 This question has rarely been addressed in *Nautilus*, though 237
238 the allometric relationships between body and shell growth 238
239 during sexual maturation has been reported in *N. pompilius* 239
240 (57). In ammonites the allometric relationships between body 240
241 and shell growth may be manifested by sometimes considerable 241
242 variations in body chamber length during development (28), 242
243 that however did not prevent these animals from regulating 243
244 their buoyancy, probably due to a flexibility of the mechanisms 244
245 of buoyancy regulation as in *Nautilus* (58). Our objective is to 245
246 first investigate whether a mismatch between body and shell 246
247 growth might account for the symmetry breaking observed 247
248 in some ammonites, and then to analyse whether the same 248
249 methodology can consistently explain the helicospiral shell 249
250 form in gastropods. 250

251 As shown in Fig. 2, we model the mollusk body by two 251
252 elastic rods, one for the ventral side of the animal, and one 252
253 for the dorsal side. The reference shape of the growing body, 253
254 i.e. the shape that the soft animal would take if it were 254
255 removed from its shell, is given by the unstressed shape of 255
256 these elastic rods, defined by their stress-free reference length 256
257 and curvature that both evolve throughout development. For 257
258 ammonites, the natural choice is to assume that the stress- 258
259 free shape is a planar logarithmic spiral, for which the *growth* 259
260 *rates* of the ventral and dorsal sides must be unequal: the 260
261 ventral side is always growing at a higher rate than the dorsal 261
262 side to ensure that they form a spiral. However, when the 262
263 body occupies the shell, the elastic rods are constrained to 263
264 match the shape of the shell tube that has been so far secreted. 264
265 The shell shape is determined by both the orientation of the

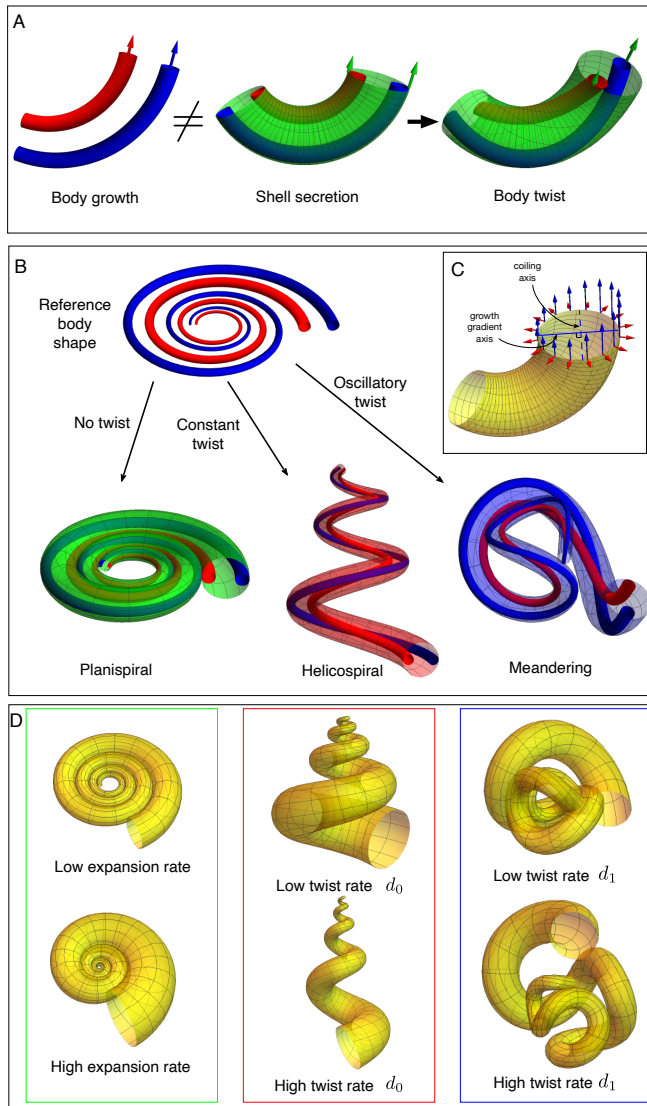


Fig. 2. Model schematic. A. A mismatch between the growth rate of the body (idealized by dorsal and ventral elastic rods) and the secretion of the shell generates mechanical stress in the animal's body that may be partially alleviated by twisting of the body within the shell tube. B. Three self-similar (i.e. with isometric growth) shell types may be generated from the same secretion parameters: if no twist, a planispiral shell; with constant twist, a helicospiral shell; with oscillatory twist, a meandering shell. C. Planar coiling geometry is captured by two parameters, an expansion rate c_1 (red arrows) and coiling gradient c_2 (blue arrows). The coiling gradient (solid line) follows the dorso-ventral axis, and generates coiling around the orthogonal axis (dashed line). D. Representative shells for the 3 shell types.

the center line of the shell. Since the growth gradient follows the dorso-ventral axis, the axis about which the shell coils (dashed line in Fig 2C) will also rotate and thus the shell shape will change; in particular, any twist will by construction generate a non-planarity to the center line curve of the shell, i.e. twisting of the animal creates torsion[†] in the shell shape.

There is an interesting feedback at work: the shape of the shell that has been so far secreted dictates the stress in the animal within the tube; mechanical stresses generate a twist of the animal body; and the orientation of the animal dictates the subsequent shape of the shell, which will, in turn create stresses on the growing animal. This two-way coupling between body shape and shell shape makes the problem particularly difficult to solve in general. Here, our approach is to exploit self-similarity, (i.e. isometric growth), which enables us to decouple the influence of mechanical stress on shell shape, and to examine the conditions under which the animal may be predicted to secrete one of three classes of shell: (i) planispiral, (ii) helicospiral, or (iii) meandering. These three shell types can be produced with equivalent secretion rates; the only difference being the orientation of the secretion given by the twisting of the animal within the shell. In particular, there is no twist in the case of the planispiral shell, a constant twist rate (with respect to whorl) for the helicospiral, and an oscillatory twist rate in the case of the meandering shell – see Fig. 2B. Therefore, assuming that the secretion rates and body growth rates are given, and that the only degree of freedom is the twisting, we can posit that the degree and form of twist by the animal will be the one that minimizes the mechanical energy of the contorted body; and thus the shell actually produced by the animal is the one corresponding to that energy-minimizing twist. With the assumption of self-similarity, we do not need to solve for the shape at each point in time based on the current orientation, rather we find an energy-minimizing twist for a single (arbitrary) time point, and the self-similar assumption implies that the same twist will be selected throughout development.

The analysis above requires a description of the shell geometry, a characterisation of the internal energy for the soft body, and a procedure for energy minimization. Full details are provided in the SI; below we briefly outline the modeling components.

A. Geometry. The geometry of the shell can be described by a set of only 5 parameters (see SI Sec. 2), $\{c_1, c_2, d_0, d_1, d_2\}$ illustrated in Fig. 2C,D. Here c_1 describes the aperture expansion rate, c_2 describes the growth/secretion gradient, i.e. the difference in growth/secretion between the ventral and dorsal sides, that produces coiling, and the parameters d_i characterise twisting. In particular, d_0 describes a constant twist, while d_1 and d_2 are, respectively, the amplitude and frequency of an oscillatory twist – equivalently, these correspond to an oscillation in the torsion of the shell centerline. In terms of these parameters, a planispiral shell corresponds to setting $d_0 = d_1 = d_2 = 0$; a helicospiral shell is constructed by setting $d_1 = d_2 = 0$, with $d_0 \neq 0$, and a meandering shell is constructed by setting $d_0 = 0$, with d_1 and d_2 both non-zero (in each case c_1 and c_2 should be non-zero). Representative shells are shown in Fig. 2D, with parameters provided in SI

[†] By torsion we refer to the mathematical definition of a measure of the twisting out of the plane of curvature of a space curve.

265 animal within the shell and the *secretion rates*. Naturally, the
 266 secretion rate on the ventral side is higher than on the dorsal
 267 side. If the secretion rates exactly match the body growth
 268 rates, then the shell shape will exactly match the logarithmic
 269 spiral shape of the body – in this case the body is always
 270 in its reference shape, and no stress will be induced in the
 271 animal. If, however, the secretion rates do not exactly match
 272 the body growth rates, mechanical stress will be induced in
 273 the mollusc body, potentially forcing the body to twist within
 274 the shell to partially relieve these stresses (Fig. 2A – see also
 275 Supplementary Information (SI) Sec 1). If the animal twists
 276 within the shell, then the dorso-ventral axis will rotate about

335 Sec. 2E. In summary, the shell shape is characterised by one
336 of the following parameter sets:

- 337 • Planispiral: $\mathcal{S}_p = \{c_1, c_2\}$
- 338 • Helicospiral: $\mathcal{S}_h = \{c_1, c_2, d_0\}$
- 339 • Meandering: $\mathcal{S}_m = \{c_1, c_2, d_1, d_2\}$

340 Our model is premised on the distinction between the geom-
341 etry of the shell and the geometry of the body. When
342 considering a bilaterally symmetric body, as with ammonites,
343 the reference shape of the body is assumed to be planar, i.e.
344 there is no intrinsic twist; thus the body is described by only
345 two parameters, $\hat{\mathcal{S}} = \{\hat{c}_1, \hat{c}_2\}$, where we use the overhats to
346 denote a reference quantity for the body. A mismatch be-
347 tween shell and body shape is then captured by any difference
348 between $\{c_1, c_2\}$ and $\{\hat{c}_1, \hat{c}_2\}$, while any twist of the body is
349 described by the parameters $\{d_0, d_1, d_2\}$. However, another
350 type of mismatch between body and shell may occur: the
351 animal may be growing in such a way as to match the shell
352 shape it is secreting, but at a faster or slower rate. This type
353 of mismatch is accounted for by a scaling parameter ξ of arc
354 length between the body and shell:

$$355 \quad \hat{t} = \xi t, \quad [1]$$

356 where \hat{t} is the arc length of the centerline corresponding to
357 the body, t is arc length attached to the shell, $\xi > 1$ means
358 the body is growing faster than the shell and conversely, for
359 $\xi < 1$, the shell is growing faster.

360 **B. Mechanical energy.** Given a set of parameters for both the
361 shell and the body, we constrain the body to fit in the shell
362 with the dorsal and ventral elastic rods situated on opposing
363 sides of the shell tube and the ventral rod following the point
364 of longest arc length. We then compute the mechanical energy
365 in each of the rods by summing the energy contributions due
366 to stretching, bending, and twisting (for details see SI Sec. 3),
367 employing a standard quadratic energy, with particular care
368 required to account for the difference in arc length between
369 the centerline of the shell tube and the ventral and dorsal
370 sides.

371 **C. Energy minimization.** Initially, we assume that the body
372 growth and secretion rates are fixed through development for
373 a given specimen, with the only degree of freedom being the
374 twisting of the animal within the shell. This assumption is
375 a sufficient and necessary condition for construction of a self-
376 similar shell. Though we note this is at best an approximation:
377 the growth and secretion vary to some degree in most shells
378 (We explore in Section E below the consequence of a variation
379 through development in these rates). Therefore, we fix the
380 body parameters $\hat{\mathcal{S}} = \{\hat{c}_1, \hat{c}_2\}$, the shell parameters $\{c_1, c_2\}$,
381 and the stretch mismatch factor ξ . We also require defining
382 the values of stiffness moduli $\{K_1, K_2, K_3\}$ which characterize
383 the resistance to stretching, bending, and twisting of the body,
384 respectively. The energy \mathcal{E} can then be expressed as a function
385 only of twisting (SI Sec. 3B), i.e.

$$386 \quad \mathcal{E} = \mathcal{E}(d_0, d_1, d_2).$$

387 For the planispiral shell, there is no twist, and the energy is
388 $\mathcal{E}_p = \mathcal{E}(0, 0, 0)$. The helicospiral shell has energy $\mathcal{E}_h(d_0) =$
389 $\mathcal{E}(d_0, 0, 0)$. As discussed in SI Sec. 3C, the most consistent

390 approach to energy minimization is to fix d_2 ; based on geomet-
391 ric considerations we fix the oscillation frequency as $d_2 = 0.8$
392 and define the meandering shell energy $\mathcal{E}_m(d_1) = \mathcal{E}(0, d_1, 0.8)$.
393 The energy landscape is complex, varying both with the shell
394 type and degree of mismatch imposed between body growth
395 and secretion. Conceptually, the case that is of most interest
396 is when the body growth rate exceeds the secretion rate, which
397 causes the animal's body to be in compression. In this case,
398 by examining the 3 components of the energy (see SI Sec. 3E),
399 a general trend emerges that shows there are values of the
400 stiffness parameters K_i for which any of the three shell types
401 can be an energy minimizer if sufficient compression is gener-
402 ated. The other case, secretion outpacing the body growth,
403 requires the body to stretch during shell secretion; then the
404 body will be in tension, and in such cases the planar shell was
405 always found to be the energy minimizer.

406 To demonstrate this range of energy minimizers, we portray
407 the energy landscape via a morphological phase space in Fig. 3,
408 constructed by fixing the geometric parameters, with a small
409 degree of imposed mismatch, then sweeping over a range of
410 mechanical parameters and determining for each parameter
411 choice the shell with the minimum energy. Two such plots ap-
412 pear in Fig. 3, with the energy-minimizing shell type denoted
413 by color: green for planispiral, blue for meandering, and red
414 for helicospiral. The coiling parameters $\{\hat{c}_1, \hat{c}_2, c_1, c_2, \xi\}$ are
415 chosen to correspond to sample values for a typical planispiral
416 (Fig. 3A) and meandering (Fig. 3B) shell. We then sweep
417 over the mechanical stiffness ratios K_1/K_2 and K_3/K_2 . For
418 instance, a point in the lower right corner denotes a body with
419 mechanical structure that has high resistance to stretching but
420 low resistance to twisting. In both cases, stiffness ratios exist
421 for which each of the three shell types is predicted. In partic-
422 ular, when the parameters correspond to a typical planispiral
423 shell, the planispiral shell type is the energy minimizer for
424 most stiffness ratios, while when the coiling parameters corre-
425 spond to sample values for a meandering shell (Fig. 3B) with
426 two different coiling gradients, the heteromorph shell types
427 are energy minimizers for a much wider range of parameter
428 space.

429 It is important to note that we did not include the steric
430 constraint that prohibits self intersection of the shell tube with
431 previous whorls. This means that some of the mechanically
432 favorable shells are not geometrically possible. In particular, in
433 Fig. 3B the planispiral shell has significant overlap. While some
434 degree of overlap is a feature found in almost all planispiral
435 ammonites (see Sec. 3), it is interesting to observe that with
436 the secretion rates such that the overlap leaves little room
437 for the mollusk body in the planispiral shell tube, there is a
438 significant increase in mechanical favorability of the twisted,
439 non-overlapping, shells.

440 **D. Data comparison.** Our model assumes that heteromorph
441 ammonites emerge due to a mechanically induced twisting
442 of the body, meaning that at the level of body growth and
443 secretion, there is no difference between these shells and the
444 far more typical planispiral ammonite. This feature enables
445 us to test the model quantitatively: for each choice of coil-
446 ing parameters $\{\hat{c}_1, \hat{c}_2, c_1, c_2, \xi\}$, we define the likelihood of
447 finding a meandering or helicospiral shell by sweeping over
448 possible stiffness ratios, and determining the percentage of
449 parameter space for which each shell type is an energy mini-
450 mizer. Such a calculation appears in Fig. 4A. Here we have

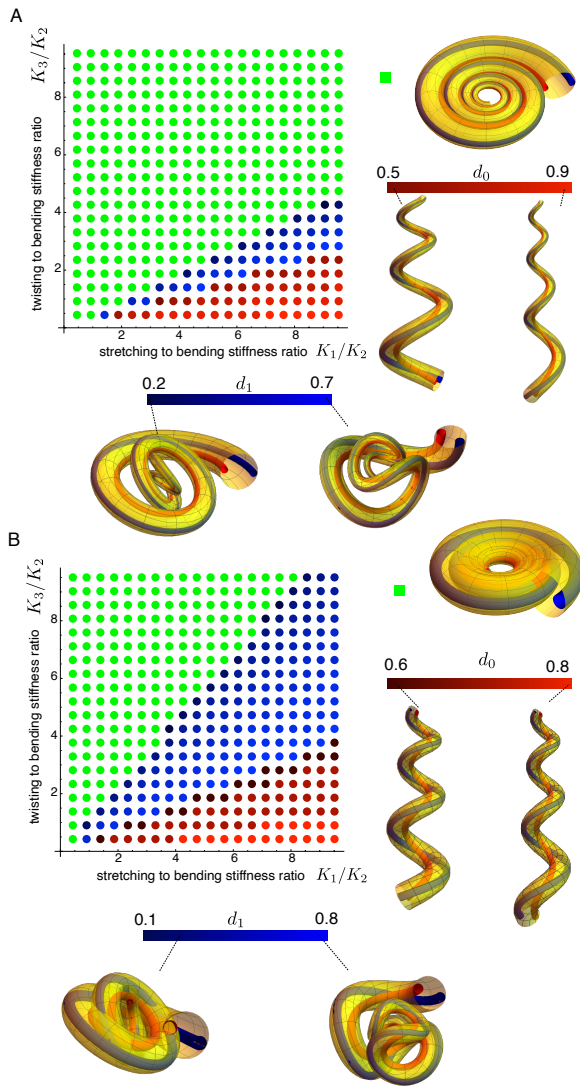


Fig. 3. Morphological phase space, sweeping over stiffness ratios K_1/K_2 (stretching to bending) and K_3/K_2 (twisting to bending). For each value of stiffness ratios, the energy minimizing shell type – planispiral (green), helicospiral (red), or meandering (blue) – is computed, with energy minimizing coiling values and corresponding shell forms indicated by colorbar. The shells in each phase space have equivalent coiling and expansion parameters, matching those in the planar green shell, differing only in the type and degree of twist. Body growth and secretion values are (A): $\hat{c}_1 = 0.02$, $\hat{c}_2 = 0.2$, $\hat{d}_0 = 0$, $c_1 = 0.02$, $c_2 = 0.25$, $\xi = 1.0$, and (B): $\hat{c}_1 = 0.02$, $\hat{c}_2 = 0.323$, $\hat{d}_0 = 0$, $c_1 = 0.02$, $c_2 = 0.4$, $\xi = 1.0$.

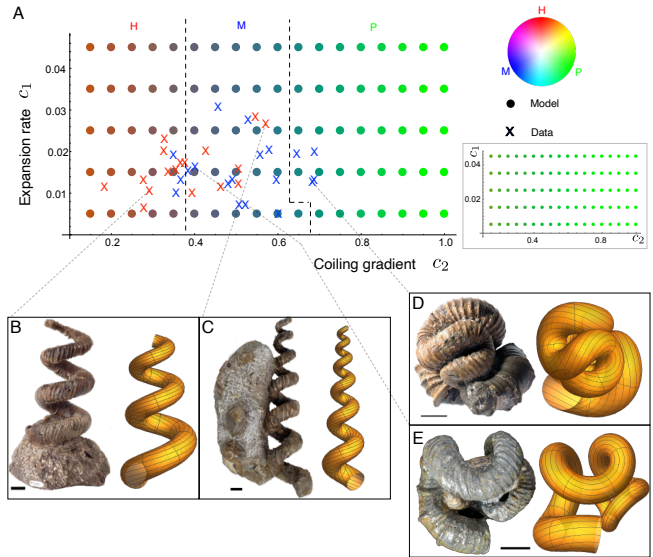


Fig. 4. (A) A phase space of coiling parameters is created by sweeping over mechanical stiffness ratios and computing the energy minimizing shell, then coloring the point using RGB value corresponding to the percent of energy minimizers of each type – planispiral=green, helicospiral=red, meandering=blue. Data points for 19 meandering and 17 helicospiral shells are plotted using extracted coiling parameters. Inset: a phase space with decreased compression factor. (B)-(E): sample shell images (Scale bars, 10 mm) and simulated shells with extracted parameters, corresponding to the indicated points.

$c_2 \lesssim 0.4$, while for large coiling gradient, the planispiral shell is by far the most likely shape. To test these predictions, we have extracted the coiling parameters (c_1, c_2) from a set of 19 meandering (*Nipponites mirabilis*) and 17 helicospiral shells (*Eubostrychoceras japonicum*). These appear as the red and blue data points in Fig. 4A, and show broad agreement with the model prediction. The best fit shells for the indicated data points appear in Fig. 4B-E; shells (real and simulated) for all data points and all extracted parameter values are provided in SI Sec. 4.

While Fig. 4 provides strong evidence in favour of the mechanical twisting hypothesis, we must be careful with its interpretation. It would be incorrect to conclude that planispiral ammonite shells are only likely to be found on the right side of the diagram, as in fact planispiral ammonites may be found over the entire range of the coiling parameters. Here we emphasize that the twisting only occurs if there is a mismatch between body growth and shell secretion, characterized in this calculation by setting $\xi = 1.075$, meaning that the reference shape of the body is 7.5% longer than the shell tube it is secreting. Without some form of mismatch the body is stress free in the planar state and thus the planispiral shell is always mechanically favorable. Even with a reduced mismatch, the regions in which meandering and helicospiral shells are predicted become much smaller: a sample morphospace with ξ decreased to 1.025 is shown as the inset in Fig. 4; here the planispiral shell is the most favorable shape for all values of coiling parameters. The model thus predicts that most ammonites secreted a planispiral shell due to low or no mismatch. It is for this reason that we do not include data points for planispiral shells in Fig. 4; the point of the computation is not to predict the presence of planispiral shells, but rather to predict where heteromorph shells will appear when the

498 necessary ingredient of a mismatch is present.

499 **E. Varying shell type through development.** Observe that the
500 twisting parameters do not appear in Fig. 4. Thus, while the
501 helicospiral and meandering shells occupy much of the same
502 region of the coiling parameter space, the difference in form
503 comes from the simple difference between a constant twist rate
504 in the case of the helicospiral shell and an oscillatory twist
505 in the case of the meandering shell. It is worth highlighting
506 that such distinctively different forms may be mechanically
507 favorable in the same region of this (2D) coiling space; which
508 may explain why some shells display both types of coiling
509 at different life stages (59) and why *Nipponites* shares many
510 diagnostic characteristics with the coexistent *Eubostriochoceras*
511 from which it derives (35).

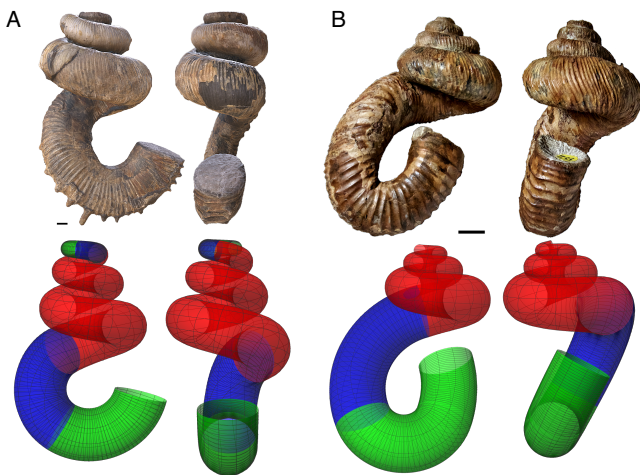


Fig. 5. Simulation and images of (A) *Didymoceras nebrascense* and (B) *Nostoceras malagasyense*, obtained by varying the mismatch and stiffness parameters during development, causing transitions in development between planispiral (green), meandering (blue), and helicospiral (red). Scale bars, 10 mm. Shell specimen info and other model parameters provided in SI.

512 In our model, a transition in shell form can be generated by
513 a change in mismatch and/or stiffness parameters during devel-
514 opment. This is demonstrated in Fig. 5, in which we provide
515 simulations of *Didymoceras nebrascense* (A) and *Nostoceras*
516 *malagasyense* (B). The shell in (A) was obtained by first vary-
517 ing the arc length mismatch parameter ξ , causing a transition
518 in the juvenile stage from planispiral to meandering to heli-
519 cospiral; and then varying the coiling and stiffness parameters
520 in the late stage of development, which generates the reverse
521 transition from helicospiral to meandering to planispiral (see
522 details in SI Sec. 5). A similar transition produces the shell
523 in (B), though without the juvenile transition missing due to
524 breakage in our specimen. Although we can only speculate
525 on the biological significance of these parameter changes, it
526 should be noted that shell coiling changes in the last stages of
527 development of many ammonites are associated with sexual
528 maturation, which in *Nautilus*, are associated with modifica-
529 tions of growth of the shell and body parts (60). Our study
530 of heteromorph ammonites illustrates also the clear difference
531 between a purely geometric simulation of shell coiling and a
532 model that includes explicitly developmental mechanisms and
533 physical constraints. Indeed, while it is possible to simulate a
534 developmental transition between a helicospiral and planispiral

stage with coaxial coiling, our model shows that this coaxi- 535
ality is mechanically unlikely. As evident in Figs 3 and 4A, 536
and demonstrated more thoroughly in SI Sec. 6, the regions 537
of parameter space in which the helicospiral and planispiral 538
shells are mechanically favorable are always separated by a 539
region in which the meandering shell is favorable. Therefore, 540
if a change in shell type occurs during development due to a 541
continuous change in parameters, our model predicts that a 542
transition from helicospiral to planispiral must always pass 543
through an intermediate meandering stage which, by construc- 544
tion, will reorient the coiling axis. This rule is consistent with 545
the fact that, to our knowledge, helicospiral and planispiral 546
stages are never strictly coaxial in heteromorph ammonites, 547
the coiling axes can even be at right angles to each other 548
(Fig. 1B,E). This prediction is an example of a developmental 549
constraint imposed by mechanics of morphogenesis (see (9) for 550
a discussion of this concept). 551

3. A new twist on shell coiling 552

Although heteromorph ammonites with chiral shells represent 553
only about 1% of 3000 genera, their geometric diversity sur- 554
passes that of the other ammonites, which probably lies in the 555
fact that they have non-overlapping whorls. In gastropods, a 556
whorl partially dictates the growth path of the next overlap- 557
ping whorl (61, 62). The mantle secretes an overlapping layer 558
on the previous whorl to which it adheres and when this at- 559
tachment zone is partially or totally lost, the coiling geometry 560
is quantitatively modified (63). Whorl overlap played a role in 561
ammonites too (64) and in some way, constrained the range 562
of possible morphologies in restricting the degrees of freedom 563
of the growing system. For instance, a shell of the kind of 564
Didymoceras generated by different coiling geometry during 565
development, could not be achieved with overlapping whorls. 566
But then, what are the regulation mechanisms of shell coiling 567
in the non-overlapping case? 568

Since mollusk shells are incrementally secreted along their 569
opening edge, it seems logical that their coiling geometry could 570
be fully understood in light of growth regulating processes 571
localized at the secreting mantle edge only. This idea has 572
motivated all theoretical models of shell coiling and experi- 573
mental approaches as well, but is confronted with an issue 574
especially obvious in the case of heteromorph ammonites. One 575
puzzling aspect of their morphogenesis is indeed the mecha- 576
nisms that govern the three-dimensional path followed by the 577
secreting mantle edge, resulting in highly convoluted forms. 578
Theoretical models predict that an incremental rotation of the 579
growing front underlies the development of helicospiral shells 580
(45, 65, 66). Yet, to our knowledge, no mechanism localized at 581
the mantle edge can trigger this movement. Our model sug- 582
gests that this incremental rotation may be naturally triggered 583
by a mechanical twist of the body, resulting from a mismatch 584
between body and shell growth. An important conclusion 585
may then be drawn from the study of these heteromorph am- 586
monites: although the form of the shell corresponds only to 587
a spatiotemporal record of accretionary growth at its edge, 588
the three dimensional path followed by the secreting mantle 589
edge is partly governed by the mechanics of the body inside 590
the shell. Whereas, it is now clear that some ornamentation 591
patterns in mollusk shells emerge as the result of mechanical 592
forces at the secreting mantle margin (8, 9, 51–54), our study 593
shows that the mechanical interactions between body and shell 594

595 may also play a key-role in the regulation of shell coiling.

596 This mechanical hypothesis explains a number of puzzling
597 characteristics of these ammonites, notably how they secreted
598 asymmetric shells while keeping a bilaterally symmetric body
599 diagnostic of cephalopods. With the same bilaterally sym-
600 metric growth gradient at the shell edge, an asymmetric or
601 symmetric shell may be secreted depending on whether the
602 bilaterally symmetric body is twisted or not. This mechanical
603 twist is recorded by the angular offset between the ventral
604 siphuncle in the posterior part of the body chamber and the
605 anterior ventral zone toward the shell edge (67). In a sinistral
606 *Turrilites*, the ventral siphuncle is shifted toward the right side
607 of the shell tube, while dorsal muscle scars are shifted toward
608 the opposing left side (see (68) pl.18 fig.1-3). This mechanical
609 twist explains also why asymmetric shells may develop after
610 hatching, well after organogenesis and the formation of the
611 plane of bilateral symmetry of the body. Further, the modifica-
612 tions of shell symmetry during development such as the shifts
613 seen in some genera from bilaterally symmetric, to asymmetric
614 and to symmetric again, reflect changes in mechanical strains
615 affecting the bilaterally symmetric body. The fact that hetero-
616 morph ammonites with asymmetric shells have repeatedly
617 evolved from ancestors with bilaterally symmetric shells is also
618 consistent with this ahistorical generic mechanism.

619 In our model, the mechanical energy is equivalent for twist-
620 ing in either direction. A twist of a bilaterally symmetric
621 body is thus consistent with a random, non-heritable direc-
622 tion of shell handedness, with right and left-handed coiling
623 arising with equal probability. However, representatives of
624 the family Turritidae (Fig. 1A) show another puzzling evo-
625 lutionary trend to our knowledge unique in the fossil record,
626 and that may be interpreted for the first time in light of our
627 approach. In the genus *Mariella* from South Africa and Texas,
628 Albian species are dextral or sinistral in a 50/50 ratio while all
629 Cenomanian species are sinistral (38, 69). Thus, directional
630 asymmetry arose from ancestors where left-right asymmetry
631 was random. Similar evolutionary patterns in current phal-
632 lostethid fishes and fiddler crabs have been interpreted as
633 an “unconventional mode” of evolution (“phenotype precedes
634 genotype”), the idea being that phenotypic variation (right
635 or left-handed) arose before genetic mechanisms controlling
636 a given direction of asymmetry (39). But this interpretation
637 depends on the way phenotypic characters are defined. Me-
638 chanical forces may generate helicospiral coiling, and though
639 they are growth dependent and modulated by genetic and
640 molecular processes so that their outcome cannot be described
641 as “phenotype first”, they may equiprobably produce dex-
642 tral or sinistral forms. Directional asymmetry, on the other
643 hand, requires a consistent bias toward one side, as in physical
644 systems generating helices (70). In light of randomization
645 of visceral asymmetry in mutant mice, an original two com-
646 ponents abstract system has been proposed to explain how
647 left-right asymmetry might arise in Bilateria (71): a generic
648 process (a reaction-diffusion system in the original hypothesis)
649 producing random asymmetry at the cellular and multicellular
650 level, can be consistently biased toward a direction by a mech-
651 anism that converts molecular to cellular asymmetry. Likewise
652 the fixation of sinistral shells in Turritidae can be interpreted
653 in light of a two components process: a generic, mechanical
654 process generating helicospiral shells with no preferred hand-
655 edness in ancestral forms, and another one (that unfortunately

will remain unknown) introducing a bias toward the leftward
coiling in descendant species. An analogous situation has been
described in the case of cardiac development in amniotes in
which a buckling instability twists the straight cardiac tube
into a helical loop with random handedness, while molecular
and cellular mechanisms introduce a bias that, except in rare
mutants, consistently triggers a rightward looping (72).

Finally, our approach may explain the development of rare
paleozoic nautiloids with helicospiral shells (73). It may also
shed new light on abnormal shell growth in ammonites with
whorls overlapping, although the mechanical influence of this
trait, probably dependant on the degree of overlapping, is
not included in our model due to the additional theoretical
difficulties that it would raise. In *Nautilus*, epizoans growing
fixed on the outer surface of the shell may perturbate the
growth of the next whorl, slowing or inhibiting the forward
movement of the animal’s body (74), a process that could
generate compression in the growing body. Our model suggests
that this compression may generate meandering or helicospiral
shells, similar to the abnormal forms described in slightly
overlapping planispiral ammonites encrusted by epizoans (75).

4. How snails coil their shell

Much progress has been made on the genetic and molecular
processes that set the left or right handedness of the asym-
metric body in snails, but an important point rarely acknowl-
edged is that the mechanisms underlying the development
of helicospiral shells themselves remain poorly understood.
First, the link between the body and shell handedness is not
straightforward, contrarily to what may be reported in light
of the development of the model organism, the pond snail
Lymnaea. This genus is orthostrophic, which means that the
body handedness corresponds to the shell handedness. But
in hyperstrophic species, anatomically dextral animals have
sinistral shell and *vice versa*, while in more complex cases
called heterostrophy, shell handedness changes after hatching
(76). Moreover, although limpets show a dextral cleavage pat-
tern, a right expression of *nodal* (22), and are right-handed in
their body anatomy, both their embryonic and post-embryonic
shell is cone-shaped and bilaterally symmetric (77). The asym-
metric development of gastropods is further complicated by a
rotation which occurs during larval development and which
moves the visceral mass, mantle, and shell at 180° with respect
to the head and foot (this rotation is, confusingly, referred to
as “torsion” in the literature but does not describe the coiling
torsion of the shell). But this process cannot be unequivocally
linked to helicospiral coiling since limpets also experience such
a rotation (78). Furthermore, a left/right asymmetric gradient
of the Dpp (decapentaplegic) protein (79) or an asymmet-
ric cellular growth pattern in the mantle edge (80) cannot
explain the incremental rotation of the growing front generat-
ing helicospiral shells. Comparative anatomy of limpets and
helicospiral species suggests a possible mechanism.

In helicospiral species, the shell-muscle system is helically
coiled around and anchored to the axial columella of the
shell three-quarters to two whorls back from the aperture,
and extends into the foot (81). In cone-like limpets, muscle
runs dorso-ventrally and attaches to the inner shell surface
in a horseshoe-shaped muscle scar bilaterally symmetric on
both sides of the body (82). While “true limpets” belong
to the order Patellogastropoda, limpet-shaped shells have

716 convergently evolved in not-closely-related species belonging to
 717 the four other gastropod orders predominantly helicospiral. In
 718 all cases, evolutionary changes from helicospiral to bilaterally
 719 symmetric limpet-shaped shells are correlated with a drastic
 720 modification of the shell-muscle system, from a coiled muscle
 721 attached on one side to the axial columella of the helicospiral
 722 shells, to a horseshoe-shaped muscle bilaterally symmetric on
 723 both sides of the body typical of true limpets (82–84). These
 724 repeated modifications of both shell coiling and muscle-shell
 725 system during evolution suggest that both characters could
 726 be developmentally correlated, and that bilateral asymmetry
 727 of the muscle-shell system could induce a twist of the body
 728 in species with helicospiral shells. Although this hypothesis
 729 remains to be tested experimentally, our theoretical framework
 730 already allows us to explore the effect of the intrinsic twist of
 731 the body on the shell form.

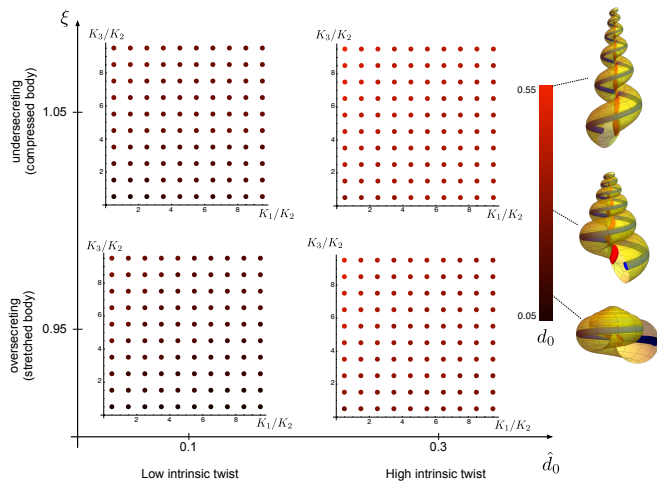


Fig. 6. Morphological phase space for gastropods for varying intrinsic twist $\hat{d}_0 \in \{0.1, 0.3\}$ and mismatch parameter $\xi \in \{0.95, 1.05\}$; with a sweep over stiffness ratios K_1/K_2 (stretching to bending) and K_3/K_2 (twisting to bending) at each point. Energy minimizing shell type is indicated by color, with red helicospiral shell the energy minimizer in every single case. Energy minimizing twisting value d_0 and corresponding shell type indicated by colorbar. Body growth and secretion values are (A): $\hat{c}_1 = c_1 = 0.06$, $\hat{c}_2 = c_2 = 0.9$.

732 **A. Modeling gastropod form.** The observations above point to
 733 the possible role of intrinsic twist, \hat{d}_0 . This parameter is geo-
 734 metrically equivalent to the helicospiral shell parameter d_0 , but
 735 is intrinsic to the animal’s body. Due to the bilateral symme-
 736 try of ammonites, $\hat{d}_0 = 0$ for all shells, while we explore in this
 737 section the mechanical consequences of $\hat{d}_0 \neq 0$ for gastropods
 738 (note that anatomically, the blue rod is anterior and the red
 739 rod is posterior in the case of a gastropod). For given body
 740 parameters $\{\hat{c}_1, \hat{c}_2, \hat{d}_0\}$ and secretion parameters $\{c_1, c_2, \xi\}$, we
 741 compute as before the effect of a mismatch by determining the
 742 energy minimizing shell. The energy minimization proceeds in
 743 the same way as outlined above, with the appropriate variation
 744 to the twisting energy (see SI Sec. 7). Naturally, in this case if
 745 there is no mismatch the animal will secrete a helicospiral shell
 746 that matches its helicospiral body shape. The question then
 747 is whether other shell types might be mechanically favorable,
 748 given a mismatch. To answer this question, we proceed as
 749 before, sweeping over a range of mechanical stiffness ratios
 750 and comparing the total mechanical energy in the planispiral

751 shell with that of the helicospiral and meandering shells for
 752 which the energy is minimum. The result appears in Fig. 6.
 753 Here we have fixed the coiling parameters, and varied both
 754 the degree of mismatch via the parameter ξ and the degree of
 755 intrinsic twist via \hat{d}_0 and plotted the resulting phase space.
 756 We find that in every single case, the helicospiral shell is the
 757 energy minimizer. We have colored each point by the energy
 758 minimizing twist value d_0 , with sample shells appearing next
 759 to the colorbar.

760 An analysis of different base coiling parameters shows that
 761 the planispiral shell can also be the energy minimizer, but
 762 only in cases of a stretched body, whereas meandering shells
 763 are never found to be favorable (see SI Sec. 7). In Fig. 7, we
 764 show the morphological phase space in the case of low intrinsic
 765 twist and $\xi = 0.95$ (stretched body) for coiling parameters
 766 matching Planorbidae, a small-sized aquatic pulmonate gastropod
 767 family. As shown in Fig. 7, the model predicts a greater
 768 likelihood of planispiral shells at low expansion rate, with the
 769 helicospiral shell being the dominant form at higher expansion
 770 rate. This trend in variation is consistently observed among
 771 Planorbidae, and was already described in 1867 in the first
 772 phylogenetic tree based on fossil evidence (85), just eight years
 773 after Darwin’s Origin of Species. Comparing Figs 3 and 7
 774 also highlights an interesting mechanical duality: tension can
 775 cause an asymmetric body to take on a symmetric shape, while
 776 compression can cause a symmetric body to take an asymmetric
 777 shape.

778 Our mechanical model predicts that in the presence of an
 779 intrinsic body twist, helicospiral shells are strongly favoured.
 780 It is well known that, once pulled out of its helicospiral shell,
 781 the body of gastropods remains helicospiral. This might seem
 782 logical since the body has grown and had to fit inside the shell.
 783 We suggest however that the body is helicospiral because
 784 it is intrinsically twisted, possibly due to the asymmetric
 785 development of the muscle-shell system, and that this intrinsic
 786 twist provides the motor for the incremental rotation of the
 787 secreting mantle edge required to generate the helicospiral
 788 shell.

789 Our approach may help to explain many aspects of shell
 790 coiling that are difficult to interpret in terms of relative growth
 791 rates at the shell edge only, such as the development of hyper-
 792 strophic or heterostrophic species (76), of heteromorph
 793 snails involving a rotation of the body inside the shell (86),
 794 of pharmaceutically induced “banana-shaped” Planorbidae (87),
 795 or of abnormal helicospiral individuals of this family found
 796 in the wild (63), among other examples. Further, our study
 797 may inform the long standing debate about the assignment
 798 of Bellerophonitida to gastropods (88, 89). These constitute
 799 an extinct order of mollusk of uncertain systematic position
 800 (Cambrian-Triassic) characterized by a planispiral, rapidly
 801 expanding shell, but interestingly displaying a pair of muscle
 802 scars symmetric on both sides of the shell (90) suggesting an
 803 untwisted body.

5. Conclusion

804 The natural world is overflowing with strikingly regular spiral,
 805 helical, and helicospiral shapes, such as keratin fibers, collagen
 806 assembly, DNA molecules, spiral bacteria, tendrils, climbing
 807 vines, seed pods, sheep horn, the cochlea and umbilical cords
 808 among others (70, 91–96). Such structures often develop as
 809 the result of fundamental mechanical forces generated by
 810

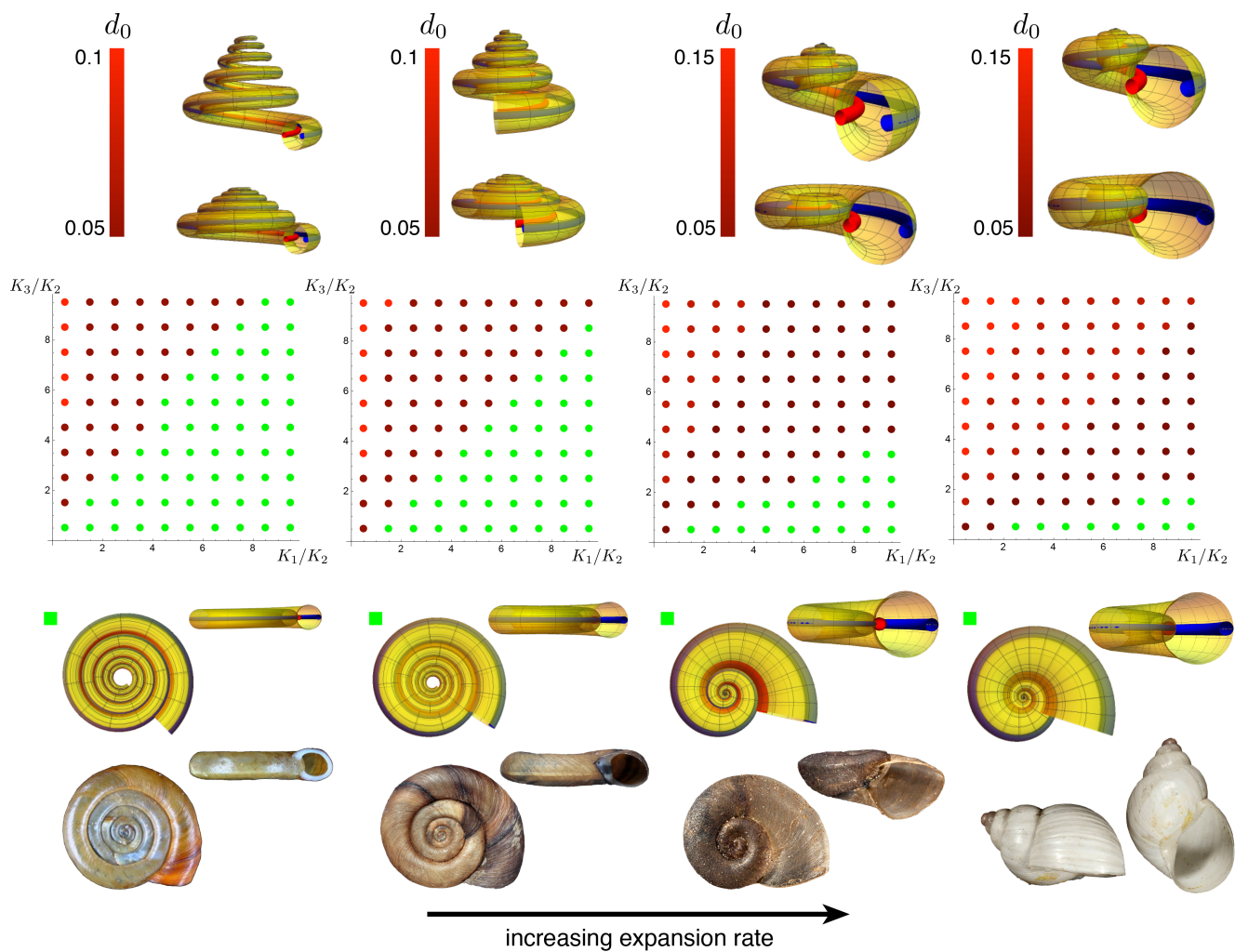


Fig. 7. A sequence of morphological phase spaces for varying expansion rate in the case of a low intrinsic twist ($\hat{d}_0 = 0.1$) and stretched body ($\xi = 0.95$) with energy minimizing shells indicated by color. The model predicts an increased likelihood of planispiral shell at lower expansion rate, characteristic of trends in Planorbidae. Coiling parameters (c_1, c_2) from left to right: (0.01,0.2), (0.02,0.37), (0.08,0.48), (0.1, 0.64). Shell images are (left to right): *Anisus leucostoma*, *Planorbis planorbis*, *Menetus dilatatus*, *Bulinus albus*.

811 a mismatch between different parts (97–99). While most
 812 previous theoretical or experimental approaches have tried
 813 to relate global shell geometry only to the growth occurring
 814 at the shell edge, our study highlights how the position and
 815 mechanics of the body inside the shell can serve to regulate its
 816 morphogenesis. Through consideration of the orientation and
 817 mechanical energy of the soft body constrained by the shell in
 818 which it resides, we have identified a basic physical mechanism
 819 that explains the origin and diversity in form of shell coiling in
 820 mollusks. This includes, in the case of ammonites, a natural
 821 explanation for the development of an asymmetric shell by a
 822 bilaterally symmetric animal, and in the case of gastropods a
 823 mechanical motor for the generation of helicospiral shells due
 824 to an intrinsic twist possibly connected to the asymmetric
 825 development of musculature. Our model also explains the
 826 meandering shells of *Nipponites*, one of the most startling
 827 forms in Nature. It would be tempting to see in this unique
 828 morphology an arbitrary quirk of evolution. In fact, similar
 829 geometric forms consisting of alternating helical sections of
 830 opposite handedness separated by multiple perversions are
 831 known to occur in bacterial shape and flagella, cellulose fibres,

832 vine tendrils and also telephone cords due to a combination of
 833 curvature-induced instability and geometric constraints (44,
 834 p. 150). In our study, the meandering form of *Nipponites*
 835 emerges as the energetically favorable path of an oscillatory
 836 twist of the animal’s body in the shell. As ammonites have
 837 been extinct for 66 million years, it is of course impossible
 838 to confirm with certainty their body symmetry. However,
 839 as we have shown that it is mechanically unfavorable for an
 840 animal with an asymmetric body to secrete a symmetric or
 841 meandering shell, our study provides strong new evidence for
 842 a bilaterally symmetric body, including in these heteromorph
 843 ammonites; this highlights the potential value of mechanics
 844 in deciphering the form of the soft body parts of a long
 845 extinct animal. Likewise, snails, which have long been used as
 846 model organisms for genetic studies, could also constitute an
 847 excellent model for studying the canalizing role of mechanics
 848 in the genesis, variation, and evolution of biological forms.
 849

Data availability. A Mathematica notebook containing model details and calculations has been deposited in the Oxford University Research Archive 850
 851
 852

855 **Acknowledgements** We are grateful to the people who
 856 provided us access to paleontological data: E. Robert, C.
 857 Salaviere (Univ. Lyon1, France), F. Giraud (Univ. Grenoble,
 858 France), D. Berthet (Mus. confluences, Lyon, France), H.
 859 Châtelier (ammonites.fr, France), C. Scheskie (Denver MNS,
 860 USA), S. Luallin, S. Jorgensen (Western Interior Pal. Soc.,
 861 USA), C. Chen (JAMSTEC, Japan), D. Aiba (Mikasa Mus.,
 862 Japan), Y. Shigeta (NMNS, Japan), H. Maeda, Y. Ito (Kyushu
 863 Univ. Mus., Japan), Y. Shiino (Pal. Soc. Japan), and C. Serra
 864 (Mus. CosmoCaixa, Spain). This work was supported by the
 865 Engineering and Physical Sciences Research Council grant
 866 EP/R020205/1

867 1. Vandenberg LN, Lemire JM, Levin M (2013) It's never too early to get it right: a conserved role
 868 for the cytoskeleton in left-right asymmetry. *Communicative & integrative biology* 6(6):12586–
 869 91.
 870 2. Inaki M, Liu J, Matsuno K (2016) Cell chirality: its origin and roles in left–right asymmet-
 871 ric development. *Philosophical Transactions of the Royal Society B: Biological Sciences*
 872 371(1710):20150403.
 873 3. Lebreton G, et al. (2018) Molecular to organismal chirality is induced by the conserved myosin
 874 1D. *Science* 362(6417):949–952.
 875 4. Juan T, et al. (2018) Myosin1D is an evolutionarily conserved regulator of animal left–right
 876 asymmetry. *Nature communications* 9(1):1–12.
 877 5. Davison A (2020) Flipping shells! unwinding lr asymmetry in mirror-image molluscs. *Trends*
 878 *in Genetics* 36(3):189–202.
 879 6. Westermann B, Schmidtberg H, Beuerlein K (2005) Functional morphology of the mantle of
 880 *Nautilus pompilius* (mollusca, cephalopoda). *Journal of morphology* 264(3):277–285.
 881 7. Jackson DJ, et al. (2006) A rapidly evolving secretome builds and patterns a sea shell. *BMC*
 882 *biology* 4(1):1–10.
 883 8. Moulton D, Goriely A, Chirat R (2015) The morpho-mechanical basis of ammonite form. *Jour-
 884 nal of theoretical biology* 364:220–230.
 885 9. Erlich A, Moulton DE, Goriely A, Chirat R (2016) Morphomechanics and developmental con-
 886 straints in the evolution of ammonites shell form. *Journal of Experimental Zoology Part B:
 887 Molecular and Developmental Evolution* 326(7):437–450.
 888 10. Wright CW (1996) Cretaceous ammonioidea. *Treatise on Invertebrate Paleontology, Part L,
 889 Mollusca 4, Revised*.
 890 11. Wiedmann J (1969) The heteromorphs and ammonoid extinction. *Biological Reviews*
 891 44(4):563–602.
 892 12. Landman NH, et al. (2012) Methane seeps as ammonite habitats in the us western interior
 893 seaway revealed by isotopic analyses of well-preserved shell material. *Geology* 40(6):507–
 894 510.
 895 13. Peterman DJ, Yacobucci MM, Larson NL, Ciampaglio C, Linn T (2020) A method to the mad-
 896 ness: ontogenetic changes in the hydrostatic properties of *Didymoceras* (Nostoceratidae:
 897 Ammonoidea). *Paleobiology* 46(2):237–258.
 898 14. Peterman DJ, Mikami T, Inoue S (2020) The balancing act of *Nipponites mirabilis* (Nosto-
 899 ceratidae, Ammonoidea): Managing hydrostatics throughout a complex ontogeny. *Plos one*
 900 15(8):e0235180.
 901 15. Van Batenburg F, Gittenberger E (1996) Ease of fixation of a change in coiling: computer
 902 experiments on chirality in snails. *Heredity* 76(3):278–286.
 903 16. Gould SJ, Young ND, Kasson B (1985) The consequences of being different: sinistral coiling
 904 in cerion. *Evolution* 39(6):1364–1379.
 905 17. Sturtevant AH (1923) Inheritance of direction of coiling in *Limnaea*. *Science* 58(1501):269–
 906 270.
 907 18. Freeman G, Lundelius JW (1992) Evolutionary implications of the mode of d quadrant spec-
 908 ification in coelomates with spiral cleavage. *Journal of Evolutionary Biology* 5(2):205–247.
 909 19. Hosoi Y, Harada Y, Kuroda R (2003) Construction of a backcross progeny collection of dex-
 910 tral and sinistral individuals of a freshwater gastropod, *Limnaea stagnalis*. *Development*
 911 *genes and evolution* 213(4):193–198.
 912 20. Shibazaki Y, Shimizu M, Kuroda R (2004) Body handedness is directed by genetically deter-
 913 mined cytoskeletal dynamics in the early embryo. *Current Biology* 14(16):1462–1467.
 914 21. Kuroda R, Endo B, Abe M, Shimizu M (2009) Chiral blastomere arrangement dictates zygotic
 915 left–right asymmetry pathway in snails. *Nature* 462(7274):790–794.
 916 22. Grande C, Patel NH (2009) Nodal signalling is involved in left–right asymmetry in snails. *Nat-
 917 ure* 457(7232):1007–1011.
 918 23. Davison A, et al. (2016) Formin is associated with left-right asymmetry in the pond snail and
 919 the frog. *Current Biology* 26(5):654–660.
 920 24. Abe M, Kuroda R (2019) The development of CRISPR for a mollusc establishes the formin
 921 *Lsd1a* as the long-sought gene for snail dextral/sinistral coiling. *Development* 146(9).
 922 25. Boletzky S (1988) Cephalopod development and evolutionary concepts. *The Mollusca*
 923 12:185–202.
 924 26. Shigeno S, Takeno S, Boletzky Sv (2010) The origins of cephalopod body plans: a geometri-
 925 cal and developmental basis for the evolution of vertebrate-like organ systems. *Cephalopods-
 926 Present and Past* 1:23–34.
 927 27. Hanlon R, Vecchione M, Alcock L (2018) *Octopus, squid, and cuttlefish: a visual, scientific*
 928 *guide to the oceans, of most advanced invertebrates..* University of Chicago Press.
 929 28. Doguzhaeva LA, Mapes RH (2015) The body chamber length variations and muscle and
 930 mantle attachments in ammonoids. In *Ammonoid Paleobiology: From anatomy to ecology*.
 931 (Springer), pp. 545–584.

29. Landman NH, Tanabe K, Shigeta Y (1996) Ammonoid embryonic development. In *Ammonoid*
 932 *paleobiology*. (Springer), pp. 343–405. 933
 30. Tanabe K, Obata I, Futakami M (1981) Early shell morphology in some upper cretaceous het-
 934 eromorph ammonites. *Transactions and proceedings of the Paleontological Society of Japan.*
 935 *New series.* (Palaeontological Society of Japan), Vol. 124, pp. 215–234. 936
 31. Druschits V (1977) The structure of the ammonitella and the direct development of am-
 937 monites. *Paleont. Jour.* 2: 188–199. 938
 32. Monks N (1999) Cladistic analysis of albian heteromorph ammonites. *Paleontology*
 939 42(5):907–925. 940
 33. Hoffmann R, et al. (2021) Recent advances in heteromorph ammonoid palaeobiology. *Bio-
 941 logical Reviews* 96(2):576–610. 942
 34. Kennedy WJ, Landman N, Cobban WA, Scott G (2000) Late campanian (cretaceous) hetero-
 943 morph ammonites from the western interior of the united states. *Bulletin of the American*
 944 *Museum of Natural History* 2000(251):1–86. 945
 35. Okamoto T (1989) Comparative morphology of *Nipponites* and *Eubostrochoceras* (creta-
 946 ceous nostoceratids). *Transactions and proceedings of the Paleontological Society of Japan.*
 947 *New series.* (Palaeontological Society of Japan), Vol.154, pp. 117–139. 948
 36. Klingner HC, Kennedy WJ, Grulke WE (2007) New and little-known Nostoceratidae and
 949 Diplomoceratidae (cephalopoda: Ammonoidea) from Madagascar. *African Natural History*
 950 3(1):89–115. 951
 37. Klingner HC, Kakabadze MV, Kennedy WJ (1984) Upper barremian (cretaceous) heteroceratid
 952 ammonites from south africa and the caucasus and their-palaeobiogeographic significance.
 953 *Journal of Molluscan Studies* 50(1):43–60. 954
 38. Klingner H, Kennedy W (1978) Turrititidae (Cretaceous Ammonoidea) from South Africa, with
 955 a discussion of the evolution and limits of the family. *Journal of Molluscan Studies* 44:1–48. 956
 39. Palmer AR (2004) Symmetry breaking and the evolution of development. *Science*
 957 306(5697):828–833. 958
 40. Yabe H (1903) Cretaceous Cephalopoda from the Hokkaido *Journal of the College of Science*
 959 *Tokyo* Vol. 20, 2: 1–45. 960
 41. Listing JB (1847) Vorstudien über topologie. *Göttinger Studien* 1. 961
 42. Clark WELG, Medawar PB (1945) *Essays on Growth and Form presented to D'Arcy Went-
 962 worth Thompson*. (Oxford University Press). 963
 43. Maxwell JC (1892) *A treatise on electricity and magnetism*. (Clarendon, Oxford). 964
 44. Goriely A (2017) *The Mathematics and Mechanics of Biological Growth*. (Springer Verlag,
 965 New York). 966
 45. Okamoto T (1988) Analysis of heteromorph ammonoids by differential geometry. *Paleontol-
 967 ogy* 31(1):35–52. 968
 46. Okamoto T (1988) Changes in life orientation during the ontogeny of some heteromorph
 969 ammonoids. *Paleontology* 31:281–294. 970
 47. Okamoto T (1988) Developmental regulation and morphological saltation in the heteromorph
 971 ammonite *Nipponites*. *Paleobiology* pp. 272–286. 972
 48. Dunstan AJ, Ward PD, Marshall NJ (2011) *Nautilus pompilius* life history and demographics at
 973 the osprey reef seamount, coral sea, Australia. *PLoS One* 6(2):e16312. 974
 49. Ambrosi D, et al. (2019) Growth and remodelling of living tissues: perspectives, challenges
 975 and opportunities. *Journal of the Royal Society Interface* 16(157):20190233. 976
 50. Hamant O, Saunders T (2020) Shaping organs: shared structural principles across kingdoms.
 977 *Annual Review of Cell and Developmental Biology* 36:385–410. 978
 51. Chirat R, Moulton DE, Goriely A (2013) Mechanical basis of morphogenesis and con-
 979 vergent evolution of spiny seashells. *Proceedings of the National Academy of Sciences*
 980 110(15):6015–6020. 981
 52. Erlich A, Howell R, Goriely A, Chirat R, Moulton D (2018) Mechanical feedback in seashell
 982 growth and form. *ANZIAM Journal* 59(4). 983
 53. Rudraraju S, Moulton DE, Chirat R, Goriely A, Garikipati K (2019) A computational framework
 984 for the morpho-elastic development of molluscan shells by surface and volume growth. *PLoS*
 985 *computational biology* 15(7):e1007213. 986
 54. Moulton DE, Goriely A, Chirat R (2010) Mechanics unlocks the morphogenetic puzzle of
 987 interlocking bivalved shells. *Proceedings of the National Academy of Sciences* 117(1):43–
 988 51. 989
 55. Lewis DE, Cerrato RM (1997) Growth uncoupling and the relationship between shell growth
 990 and metabolism in the soft shell clam *Mya arenaria*. *Marine Ecology Progress Series*
 991 158:177–189. 992
 56. Bourdeau PE, Johansson F (2012) Predator-induced morphological defences as by-products
 993 of prey behaviour: a review and prospectus. *Oikos* 121(8):1175–1190. 994
 57. Hayasaka S, Ōki K, Tanabe K, Saisho T, Shinomiya A (2010) On the habitat of *Nautilus*
 995 *pompilius* in Tanon Strait (Philippines) and the Fiji Islands. In *Nautilus The Biology and Pale-
 996 obiology of a Living Fossil*. (Springer), pp. 179–200. 997
 58. Ward PD (1987) *The natural history of Nautilus*. (Allen & Unwin). 998
 59. Matsumoto T (1977) Some heteromorph ammonites from the cretaceous of Hokkaido. *Mem.*
 999 *Fac. Sci., Kyushu Univ., Ser. D, Geol.* 23:303–366. 1000
 60. Collins D, Ward PD (2010) Adolescent growth and maturity in *Nautilus*. In *Nautilus The Bio-
 1001 ology and Paleobiology of a Living Fossil*. (Springer), pp. 421–432. 1002
 61. Hutchinson J (1989) Control of gastropod shell shape; the role of the preceding whorl. *Journal*
 1003 *of Theoretical Biology* 140(4):431–444. 1004
 62. Checa AG, Jiménez-Jiménez AP, Rivas P (1998) Regulation of spiral coiling in the terres-
 1005 trial gastropod *Sphincterochila*: An experimental test of the road-holding model. *Journal of*
 1006 *Morphology* 235(3):249–257. 1007
 63. Clewing C, Riedel F, Wilke T, Albrecht C (2015) Ecophenotypic plasticity leads to extraordi-
 1008 nary gastropod shells found on the "roof of the world". *Ecology and Evolution* 5(14):2966–
 1009 2979. 1010
 64. Ubukata T, Tanabe K, Shigeta Y, Maeda H, Mapes RH (2008) Piggyback whorls: a new the-
 1011 oretical morphologic model reveals constructional linkages among morphological characters
 1012 in ammonoids. *Acta Palaeontologica Polonica* 53(1):113–128. 1013
 65. Moulton DE, Goriely A, Chirat R (2012) Mechanical growth and morphogenesis of seashells.
 1014 *Journal of theoretical biology* 311:69–79. 1015

- 1016 66. Moulton DE, Goriely A (2014) Surface growth kinematics via local curve evolution. *Journal of*
1017 *mathematical biology* 68(1):81–108.
- 1018 67. Ward P (1979) Functional morphology of cretaceous helically-coiled ammonite shells. *Paleo-*
1019 *biology* 5(4):415–422.
- 1020 68. Crick GC (1898) On the muscular attachment of the animal to its shell in some fossil
1021 Cephalopoda (Ammonoidea). *Transactions of the Linnean Society of London. 2nd Series.*
1022 *Zoology* 7(4):71–113.
- 1023 69. Clark DL (1965) *Heteromorph ammonoids from the Albian and Cenomanian of Texas and*
1024 *adjacent areas.* (Geological Society of America) Vol. 95.
- 1025 70. Armon S, Efrati E, Kupferman R, Sharon E (2011) Geometry and mechanics in the opening
1026 of chiral seed pods. *Science* 333(6050):1726–1730.
- 1027 71. Brown NA, Wolpert L (1990) The development of handedness in left/right asymmetry. *Devel-*
1028 *opment* 109(1):1–9.
- 1029 72. Desgrange A, Le Garrec JF, Meilhac SM (2018) Left-right asymmetry in heart development
1030 and disease: forming the right loop. *Development* 145(22).
- 1031 73. Teichert C (1964) Mollusca 3. Cephalopoda General Features - Endoceratoidea - Actinocer-
1032 atoidea - Nautiloidea - Bacritoidea. *Treatise on invertebrate paleontology. Part K.* pp. 1–519.
- 1033 74. Arnold J (1985) Shell growth, trauma, and repair as an indicator of life history for *Nautilus*.
1034 *The Veliger* 27(4):386–396.
- 1035 75. Checa AG, Okamoto T, Keupp H (2002) Abnormalities as natural experiments: a morpho-
1036 genetic model for coiling regulation in planispiral ammonites. *Paleobiology* 28(1):127–138.
- 1037 76. Okumura T, et al. (2008) The development and evolution of left-right asymmetry in inverte-
1038 brates: Lessons from drosophila and snails. *Developmental dynamics* 237(12):3497–3515.
- 1039 77. Kay MC, Emler RB (2002) Laboratory spawning, larval development, and metamorphosis of
1040 the limpets *Lottia digitalis* and *Lottia asmi* (Patellogastropoda, Lottiidae). *Invertebrate Biology*
1041 121(1):11–24.
- 1042 78. Wanninger A, Ruthensteiner B, Haszprunar G (2000) Torsion in *Patella caerulea* (Mollusca,
1043 Patellogastropoda): ontogenetic process, timing, and mechanisms. *Invertebrate Biology*
1044 119(2):177–187.
- 1045 79. Shimizu K, et al. (2013) Left-right asymmetric expression of *dpp* in the mantle of gastropods
1046 correlates with asymmetric shell coiling. *EvoDevo* 4(1):1–7.
- 1047 80. Johnson AB, Fogel NS, Lambert JD (2019) Growth and morphogenesis of the gastropod
1048 shell. *Proceedings of the National Academy of Sciences* 116(14):6878–6883.
- 1049 81. Price RM (2003) Columellar muscle of neogastropods: muscle attachment and the function
1050 of columellar folds. *The Biological Bulletin* 205(3):351–366.
- 1051 82. Heller J (2015) *Sea snails. A natural history.* (Springer).
- 1052 83. Yamamori L, Kato M (2018) Morphological and ecological adaptation of limpet-shaped top
1053 shells (Gastropoda, Trochidae, Fossarininae) to wave-swept rock reef habitats. *PLoS one*
1054 13(8):e0197719.
- 1055 84. Tseng R, Dayrat BA (2014) Anatomical redescription of the limpet-like marine pulmonate
1056 *Trimusculus reticulatus* (Sowerby, 1835). *Veliger* 51(4):194–207.
- 1057 85. Rasser MW (2013) Darwin's dilemma: the steinheim snails' point of view. *Zoosystematics*
1058 *and Evolution* 89(1):13–20.
- 1059 86. Liew TS, Kok AC, Schilthuisen M, Urdy S (2014) On growth and form of a heteromorphic
1060 terrestrial snail: *Plectostoma concinnum* (Fulton, 1901) (Mollusca, Gastropoda, Diplommat-
1061 inidae). *PeerJ PrePrints* 2:e289v1.
- 1062 87. Baynes A, et al. (2019) Early embryonic exposure of freshwater gastropods to pharmaceu-
1063 tical 5-alpha-reductase inhibitors results in a surprising open-coiled "banana-shaped" shell.
1064 *Scientific reports* 9(1):1–12.
- 1065 88. Ponder WF, Lindberg DR (1997) Towards a phylogeny of gastropod molluscs: an analysis
1066 using morphological characters. *Zoological Journal of the Linnean society* 119(2):83–265.
- 1067 89. Bouchet P, Rocroi J-P (2005) Classification and nomenclator of gastropod families. *Malacolo-*
1068 *gia* 147: 1-397.
- 1069 90. Knight JB (1947) Bellerophon muscle scars. *Journal of Paleontology* pp. 264–267.
- 1070 91. Goriely A (2004) Knotted umbilical cords. In *Physical and Numerical Models in Knot Theory*
1071 *Including Their Application to the Life Sciences*, eds. Calvo JA, Stasiak A, Rawdon E. (World
1072 Scientific, Singapore), pp. 109–126.
- 1073 92. McMillen T, Goriely A (2002) Tendril perversion in intrinsically curved rods. *Journal of Nonlin-*
1074 *ear Science* 12(3):241–281.
- 1075 93. Goldstein RE, Goriely A, Hubber G, Wolgemuth C (2000) Bistable helices. *Phys. Rev. Lett.*
1076 84.
- 1077 94. Wolgemuth CW, et al. (2005) How to make a spiral bacterium. *Physical biology* 2(3):189.
- 1078 95. Goriely A, Neukirch S (2006) Mechanics of climbing and attachment in twining plants. *Phys.*
1079 *Rev. Lett.* 97(18):184302.
- 1080 96. Moulton DE, Oliveri H, Goriely A (2020) Multiscale integration of environmental stimuli in plant
1081 tropism produces complex behaviors. *Proceedings of the National Academy of Sciences*
1082 117(51):32226–32237.
- 1083 97. Lessinnes T, Moulton DE, Goriely A (2017) Morphoelastic rods. Part II: Growing birods. *J.*
1084 *Mech. Phys. Solids* 100:147–196.
- 1085 98. van Manen T, Janbaz S, Zadpoor AA (2018) Programming the shape-shifting of flat soft mat-
1086 ter. *Materials Today* 21(2):144–163.
- 1087 99. Moulton DE, Lessinnes T, Goriely A (2020) Morphoelastic rods iii: Differential growth and
1088 curvature generation in elastic filaments. *Journal of the Mechanics and Physics of Solids* p.
1089 104022.